Performance of a Novel Inerter-Based Isolation System for Medium-Rise Buildings Under Seismic and Wind Excitations

JUBIN LU and SONGYE ZHU

ABSTRACT

Base isolation is a useful technique to mitigate superstructural vibrations based on the principle of shifting structural natural frequencies lower than the dominant frequency range of seismic excitations. However, excessive displacement may be concentrated at the flexible substructure, causing the loss of its building functions. Besides, the conventional isolation systems make the building structures, especially the medium- and high-rise ones, be vulnerable to wind excitations. This paper presents a novel inerter-based isolation system and investigate its seismic isolation and wind resistance performances through a 12-story RC building model. First, the isolation principle of the inerter-based isolation system is investigated based on an equivalent 2-DOF model. Also, the optimization scheme for the inerter-based isolation system is proposed. Then, the spectral representation methods (SRM) for 1d-1v and 1d-Nv stochastic processes are utilized to generate the time history samples of seismic and wind excitations, respectively. Last, the performance of the inerter-based isolation system is evaluated in time domain. The results show that the inerter-based isolation system can achieve the comparable seismic isolation effect for the superstructure without reducing the physical stiffness of the substructure so that there are not amplified displacement. Meanwhile, the inerter-based isolation system exhibits a satisfying performance under wind excitations, which means that it is a preferable isolation technique for building structures located in both seismic and typhoon fields.

INTRODUCTION

The basic principle of the conventional isolation systems is to reduce the natural frequency of building structures away from the domain frequency range of seismic excitations. Some flexible equipment such as the lead rubber bearing and negative stiffness damper are used to reduce the physical stiffness of substructure [1,2]. However, the building structures installed with the conventional isolation systems often suffer

Jubin Lu and Songye Zhu, Department of Civil and Environmental Engineering, The Hong Kong Polytechnic University, Hung Hom, Kowloon, Hong Kong, China

extremely large displacements at the substructure and are sensitive to static and low-frequency excitations.

Inerter is a new mechanical element proposed by Smith [3] according to the analogy between mechanical and electrical networks. The amplitude of the force generated by inerter is proportional to the square of the excitation frequency while its phase is always 180 degrees different from the counterpart of the stiffness. It implies that inerter possesses the negative stiffness effect and only works for dynamic excitations. The anti-resonant effect, created by the cancellation of forces generated by inerter and stiffness, is another factor that makes inerter effective in vibration isolation These unique properties attract extensive research on the inerter-based isolation system [4]. However, the benefit of the inerter-based isolation system on civil structures is not demonstrated in previous studies because its isolation principle and effective scenarios have not been clearly presented.

This paper clarifies the benefits of the inerter-based isolation system on civil structures through a numerical study. The major contributions of this study fall in the following two aspects: (1) analysing and summarizing the basic principles of the inerter-based isolation system on the seismic isolation; (2) demonstrating its beneficial scenarios on civil structures, i.e., application on medium-rise buildings structures vulnerable to both seismic and wind excitations. The findings and conclusions in this study can guide the application of the inerter-based isolation system in civil structures.

GOVERNING EQUATION OF THE ISOLATED BUILDING MODEL

A 12-story RC building model with an additional base floor is adopted in this study. The structural parameters and approximated lump-mass model are given in Table I and Figure 1, respectively. The inerter-based isolation system is installed in the based floor (BF), which consists of an inerter m_I and a damper c_I in parallel.

The governing equation of the superstructure and substructure can be expressed respectively as,

$$\boldsymbol{M}_s\boldsymbol{I}_s\ddot{x}_b + \boldsymbol{M}_s\ddot{\boldsymbol{v}}_s + \boldsymbol{C}_s\dot{\boldsymbol{v}}_s + \boldsymbol{K}_s\boldsymbol{v}_s = -\boldsymbol{M}_s\boldsymbol{I}_s\ddot{x}_g \tag{1}$$

$$m_t\ddot{x}_b + (\boldsymbol{M}_s\boldsymbol{I}_s)^T\ddot{\boldsymbol{v}}_s + k_b x_b + (m_I\ddot{x}_b + c_I\dot{x}_b) = -m_t\ddot{x}_g \tag{2}$$

where $\boldsymbol{M}_s$, $\boldsymbol{C}_s$, and $\boldsymbol{K}_s$ are the mass, damping, and stiffness matrices of the superstructure; $m_t = \sum_{i=1}^{N} m_i + m_b$ is the total mass of the building model; m_I and c_I are the inertance and damping of the inerter-based isolation system; x_b is the displacement of the base floor, while $\boldsymbol{v}_s$ is the displacement vector of superstructure

TABLE I. STRUCTURAL PARAMETERS OF THE ISOLATED BUILDING MODEL

	Parameters (Unit)	Value
Superstructure	Floor height h_i (m)	3
	Mass of single floor m_i (kg)	8×10^4
	Lateral stiffness of single floor k_i (N/m)	1.4×10^8
	First modal damping ratio (%)	2
Substructure	Floor height h_b (m)	3.5
	Mass of single floor m_b (kg)	8×10^4
	Lateral stiffness of single floor k_b (N/m)	1.4×10^8

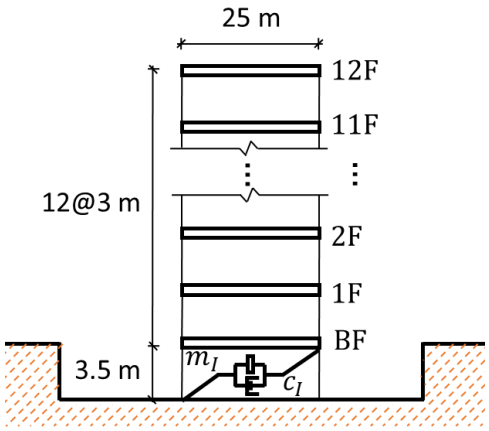

Figure 1. 12-story RC building model with inerter-based isolation system.

relative to x_b; $\ddot{x}_g$ is the seismic ground acceleration; $\boldsymbol{I}_s$ is unit vector with the dimension of N.

BASIC PRINCIPLE OF INERTER-BASED ISOLATION SYSTEM

To analyze the basic principle, the (N+1)-story isolated building model is transferred into a 2-DOF equivalent model by simplifying the superstructure as 1-DOF in terms of its 1st mode and maintaining the substructure as 1-DOF. The displacement vector $\boldsymbol{v}_s$ can be approximated by using 1st modal displacement y, i.e., $\boldsymbol{v}_s = \boldsymbol{\phi}^1 y$, where $\boldsymbol{\phi}^1$ is the 1st mode shape of the superstructure. Then, the first modal motion equation of the superstructure can be obtained by left multiplying $(\boldsymbol{\phi}^1)^T$ on both sides of Eq. (1), which can be expressed as,

$$L_1 m_e \ddot{x}_b + m_e \ddot{y} + c_e \dot{y} + k_e y = -L_1 m_e \ddot{x}_g \tag{3}$$

in which, $m_e = (\boldsymbol{\phi}^1)^T \boldsymbol{M}_s (\boldsymbol{\phi}^1)$; $c_e = (\boldsymbol{\phi}^1)^T \boldsymbol{C}_s (\boldsymbol{\phi}^1)$; $k_e = (\boldsymbol{\phi}^1)^T \boldsymbol{K}_s (\boldsymbol{\phi}^1)$;

$$L_1 = [(\boldsymbol{\phi}^1)^T \boldsymbol{M}_s \boldsymbol{I}] / [(\boldsymbol{\phi}^1)^T \boldsymbol{M}_s (\boldsymbol{\phi}^1)].$$

Combining Eqs. (2)-(3), one can obtain the governing equations of the 2-DOF equivalent model in the matrix form as,

$$\boldsymbol{m}\ddot{\boldsymbol{z}} + \boldsymbol{c}\dot{\boldsymbol{z}} + \boldsymbol{k}\boldsymbol{z} = -\bar{\boldsymbol{m}}\boldsymbol{r}\ddot{x}_g. \tag{4}$$

where, $\boldsymbol{m} = \begin{bmatrix} 1+\mu_I & L_1\mu_e \\ L_1\mu_e & \mu_e \end{bmatrix}$; $\boldsymbol{c} = \begin{bmatrix} 2\xi_I\omega_b & 0 \\ 0 & 2\mu_e\xi_1\omega_1 \end{bmatrix}$; $\boldsymbol{k} = \begin{bmatrix} \omega_b^2 & 0 \\ 0 & \mu_e\omega_1^2 \end{bmatrix}$;

$$\bar{\boldsymbol{m}} = \begin{bmatrix} 1 & 0 \\ 0 & L_1\mu_e \end{bmatrix}; \boldsymbol{z} = \begin{bmatrix} x_b \\ y \end{bmatrix}; \boldsymbol{r} = \begin{bmatrix} 1 \\ 1 \end{bmatrix}.$$

Here, $\mu_e = m_e/m_t$ is the ratio of 1st modal mass to total mass; $\xi_1 = c_e/(2m_e\omega_1)$, and $\omega_1 = \sqrt{k_e/m_e}$ are the damping ratio and natural frequency of the superstructure;

TABLE II. MODAL PARAMETERS OF THE ORIGINAL AND EQUIVALENT MODEL

Model	$\boldsymbol{\omega_1}$ **(rad/s)**	$\boldsymbol{\omega_2}$ **(rad/s)**	$\boldsymbol{\xi_1}$ (%)	$\boldsymbol{\xi_2}$ (%)
Original	4.25	6.27	2.92	3.47
Equivalent	4.25	6.28	2.92	3.48

$\omega_b = \sqrt{k_b/m_t}$ is the natural frequency of the substructure; $\mu_I = m_I/m_t$ and $\xi_I = c_I/(2m_t\omega_b)$ are the inertance ratio and damping ratio of the inerter-based isolation system, respectively.

The first two orders of modal parameters are calculated and listed in Table II. The frequencies and damping ratios of the first two vibration modes are close to those of original model, which verifies the 2-DOF equivalent approach.

Based on Eq. (4), the transfer function vectors $\boldsymbol{h}(\omega)$ can be computed as,

$$\boldsymbol{h}(\omega) = \begin{bmatrix} h_{x_b}(\omega) \\ h_y(\omega) \end{bmatrix} = -(-\omega^2\boldsymbol{m} + i\omega\boldsymbol{c} + \boldsymbol{k})^{-1}\bar{\boldsymbol{m}}\boldsymbol{r} \tag{5}$$

where $h_{x_b}(\omega)$ and $h_y(\omega)$ are the transfer functions of the seismic ground acceleration $\ddot{x}_g$ to the substructural responses x_b and the superstructural response y, respectively.

Figure 2(a)-2(b) display the features of the transfer functions $h_y(\omega)$ and $h_{x_b}(\omega)$, respectively. The inerter-based isolation system possesses the negative stiffness effect, but it would not reduce the physical stiffness of the substructure. Therefore, it can shift the natural frequency lower and will not amplify the static or low-frequency responses. Meanwhile, the anti-resonant effect, leading to an extremely low value area of the transfer functions, will be introduced between the 1st and 2nd natural frequencies, which prompts its seismic isolation effect.

Besides, Figure 3 shows that seismic and wind excitations have their unique energy distribution. The main energy of the seismic excitation concentrates on middle-frequency range near the natural frequency of the original building structure, while the main energy the wind excitation locates in the static and the low-frequency range. Therefore, the inerter-based isolation system can achieve comparable seismic isolation effect to the conventional ones, but it does not reduce the physical stiffness of the

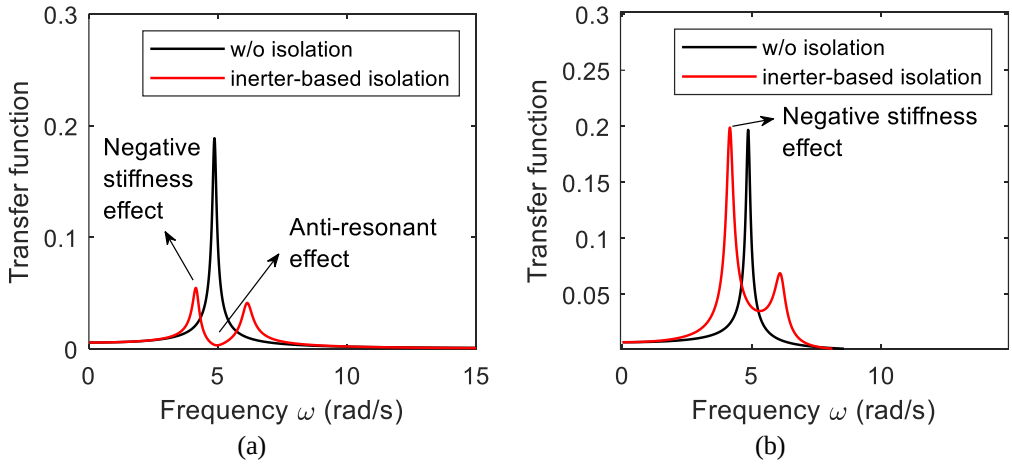

Figure 2. Transfer functions of (a) superstructure and (b) substructure. ($\mu_I = 5$ and $\xi_I = 10\%$)

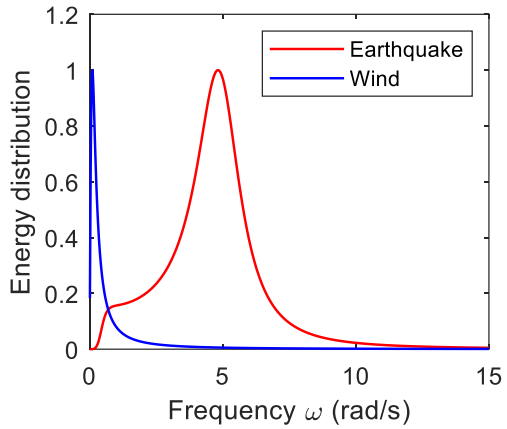

Figure 3. Energy distributions of the seismic and wind excitation.

substructure so that it will not amplify the wind-induced response.

DESIGN OF THE INERTER-BASED ISOLATION SYSTEM

It is indicated by Ye et al. [5] that there is an optimal inertance ratio for the superstructural displacement, while the substructural displacement will be continuously reduced with increase of the inertance ratio. Therefore, the parameters of inerter-based isolation system, i.e., μ_I and ξ_I, are determined by minimizing the variance response σ_y^2 of the superstructure in this study. The optimization problem can be formulated as,

$$\begin{gathered} \Delta = \operatorname{argmin}\left(\sigma_y^2\right) \\ \text{subjected to } \ 0 \le \mu_I \le \mu_{I,max};\ 0 \le \xi_I \le \xi_{I,max}; \end{gathered} \tag{6}$$

$$\sigma_y^2 = \int_{-\infty}^{\infty} \left|h_y(\omega)\right|^2 S_{\ddot{x}_g}(\omega)\, d\omega \tag{7}$$

in which, $\mu_{I,max}$ and $\xi_{I,max}$ are the upper bound of the inertance ratio μ_I and the damping ratio ξ_I.

In this study, the PSD function $S_{\ddot{x}_g}(\omega)$ of the earthquake ground acceleration $\ddot{x}_g$ is modelled by the KT spectrum as,

$$S_{\ddot{x}_g}(\omega) = \frac{\omega_g^4 + 4\xi_g^2\omega_g^2\omega^2}{\left(\omega_g^2-\omega^2\right)^2 + 4\xi_g^2\omega_g^2\omega^2} \cdot \frac{\omega^4}{\left(\omega_f^2-\omega^2\right)^2 + 4\xi_f^2\omega_f^2\omega^2} \cdot S_0 \tag{8}$$

in which, ω_g and ξ_g are the domain frequency and damping radio of the foundation soil, respectively; ω_f and ξ_f are the filter parameters; S_0 is the excitation density constant.

Here, the parameters of KT spectrum with soft soil condition are set as $\omega_g = 5$ rad/s, $\xi_g = 0.2$, ω_f=0.5 rad/s, ξ_f=0.6, and S_0=0.0113 $\mathrm{m^2/s^3}$. Based on Eq. (6), the parameters of inerter-based isolation system can be optimized as $\mu_I = 5.57$ and $\xi_I = 36\%$ by using the function *fmincon* in MATLAB.

ANALYSIS OF SEISMIC ISOLATION PERFORMANCE

In this section, the isolation performance of the inerter-based isolation system is evaluated. First, the time history of the seismic ground acceleration $\ddot{x}_g(t)$ is simulated based on the spectral representation method (SRM) for 1v-1d stochastic processes [6]. A total of 100 samples are simulated to eliminate the stochastic error. Afterwards, the time histories of the structural responses of the building structure without isolation and with the inerter-based isolation system can be calculated.

It can be found from Figures 4(a)-4(b) that the inerter-based isolation system can obviously reduce the superstructural responses of the drift and absolute acceleration at the 1st floor compared with those without control. Meanwhile, the inerter-based isolation system will not amplify the displacement at the base floor as shown in Figure 4(c).

Then, the maximum structural responses under earthquake excitation along the building height are calculated to illustrate the control effect to the entire building structure. To eliminate the stochastic error, the average values of the maximum structural responses obtained from the 100 simulated samples of $\ddot{x}_g(t)$ are used, and the results are shown in Figure 5. It can be found that the inerter-based isolation system can reduce both maximum drift and absolute acceleration responses of the entire building structure without amplifying the structural responses at the base floor.

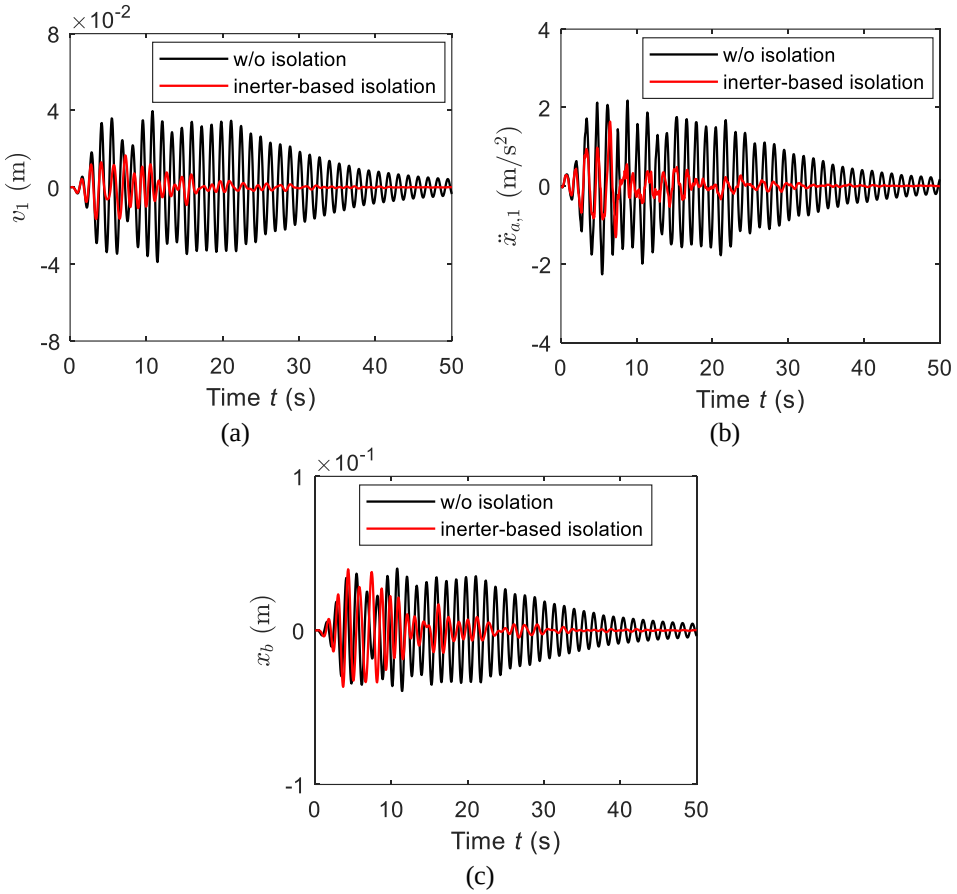

Figure 4. The time histories of the structural responses of (a) the drift at the 1st floor, (b) the absolute acceleration at the 1st floor, and (c) the displacement at the based floor.

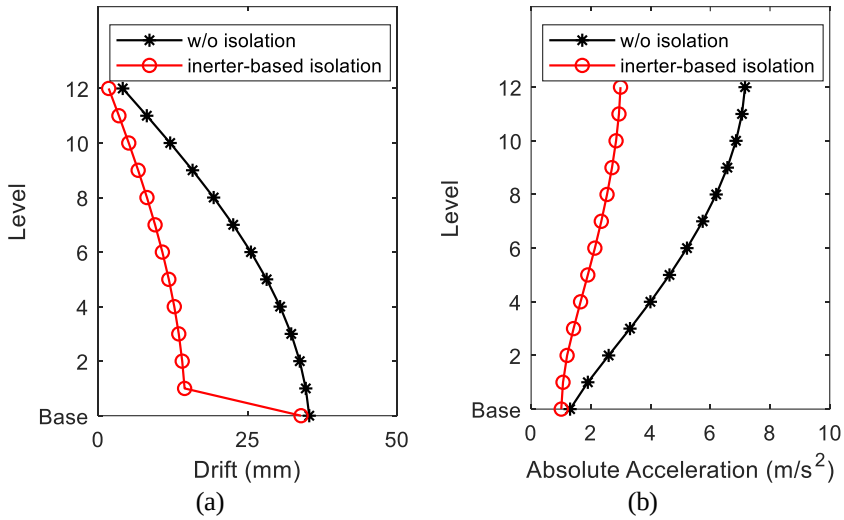

Figure 5. The maximum structural responses along the building height (a) Drift and (b) Absolute acceleration.

ANALYSIS OF WIND-RESISTANT PERFORMANCE

For the mid-rise or high-rise isolated building structures, the wind excitation might be the dominant excitation. Therefore, the performance of the inerter-based isolation system is evaluated under the wind excitations in this section.

The time history of the wind excitation $\boldsymbol{f}_w$ is artificially simulated based on SRM for 1d-Nv stochastic processes [7]. Then, the wind-induced structural response can be calculated. Figure 6 shows the structural responses on the top and base floors, from which the slight control effect of inerter-based isolation system can be found.

The displacement responses along the building height are further illustrated by the box chart as shown in Figure 7. The mean displacement responses at each floor of the building structure without control and with the inerter-based isolation system are almost equal, but the vibration range will be narrowed if the inerter-based isolation system is installed. That is because the inerter only functions for the dynamic excitation, i.e., the fluctuating wind component, but not for the static excitation, i.e., the mean wind component.

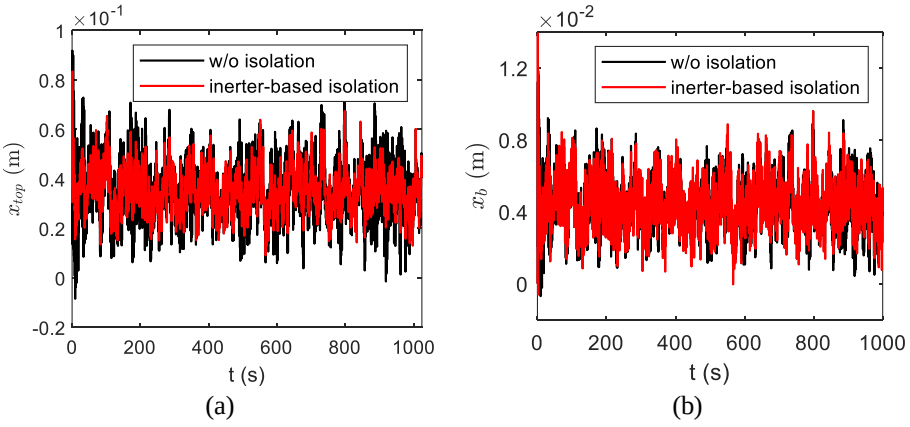

Figure 6. The displacement responses at (a) the top floor and (b) the base floor.

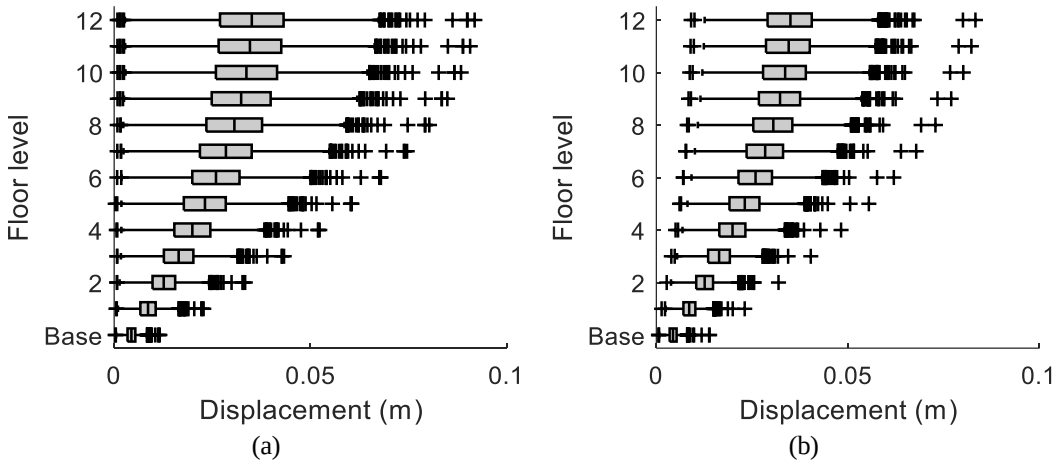

Figure 7. The displacement responses under wind excitation along the building height: (a) w/o isolation (b) inerter-based isolation.

CONCLUSIONS

This paper numerically studies a novel inerter-based isolation system with respect to its seismic isolation and wind resistance performances, aiming to clarify its basic principle and effective scenarios in civil structures. The findings and conclusions are summarized as follows:

(1) The inerter-based isolation system is beneficial form its unique negative stiffness effect and anti-resonant effect.

(2) It can achieve considerable seismic isolation effect on the superstructure but does not amplify the displacement of the substructure.

(3) Inerter only functions for the dynamic excitations so that it has control effect for the fluctuating wind component. Meanwhile, it is not vulnerable to the mean wind component as it does not reduce the physical stiffness of substructure.

REFERENCES

1. Kelly, J.M. 1999. “The role of damping in seismic isolation,” *Earthq. Eng. Struct. Dyn.,* 28:3-20.
2. Shi, X. and Zhu, S. 2019. “A comparative study of vibration isolation performance using negative stiffness and inerter dampers,” *J. Franklin Inst.,* 356:7922-7946.
3. Smith, M.C. 2022. “Synthesis of mechanical networks: the inerter,” *IEEE Trans. Autom. Control,* 47:1648-1662.
4. Kuhnert, W.M., Gonçalves P.J.P., Ledezma-Ramirez D.F., and Brennan M.J. 2021. “Inerter-like devices used for vibration isolation: a historical perspective,” *J. Franklin Inst.,* 358:1070-1086.
5. Ye, K., Shu, S., Hu, L., and Zhu H. 2019. “Analytical solution of seismic response of base‐isolated structure with supplemental inerter,” *Earthq. Eng. Struct. Dyn.,* 48:1083-1090.
6. Shinozuka M., Deodatis G. 1991. “Simulation of stochastic processes by spectral representation,” *Appl. Mech. Rev.,* 44(4):191-204.
7. Deodatis G. 1996 “Simulation of ergodic multivariate stochastic processes,” *J. Eng. Mech.,* 122:778-787.